A reinvestigation of low molecular weight components in SOA produced by cyclohexene ozonolysis

Jun Chen[1] · Zhao-Hui Li[1] · Ye-Peng Yu[1] · Xuan Lin[1] · Hang Zhang[1] ·
Yan-Bo Li[1] · Huan-Huan Wang[1] · Rui-Rui Sun[1] · Qing-Hui Meng[1] ·
Chao-Qun Huang[2] · Xiao-Bin Shan[1] · Fu-Yi Liu[1] · Chang-Jin Hu[3] ·
Wei-Jun Zhang[3,4] · Liu-Si Sheng[1]

Abstract The ozonolysis of cyclohexene is an important model system for understanding the more complex reaction of O_3 with monoterpenes; however, many previous studies have come to qualitatively different conclusions about the composition of the secondary organic aerosol (SOA) formed in this system. In the present study, the composition of the SOA produced by cyclohexene ozonolysis in the absence of seed aerosols has been investigated online and off-line using synchrotron-based thermal desorption/tunable vacuum ultraviolet photoionization time-of-flight aerosol mass spectrometry (TD-VUV-TOF-PIAMS) in conjunction with a custom-built smog chamber. On the basis of the molecular ions observed by mass spectrometry at 11.5 eV, it was found that dicarboxylic acids, dialdehydes, and cyclic anhydrides are the predominant low molecular weight components in the particle phase. The results also indicated that TD-VUV-TOF-PIAMS coupled with filter sampling is a potentially useful tool for the investigation of SOA composition both in the field and in the laboratory.

Keywords Cyclohexene · Ozonolysis · SOA · Smog chamber · Aerosol mass spectrometry

✉ Chao-Qun Huang
cqhuang@aiofm.ac.cn

✉ Fu-Yi Liu
fyliu@ustc.edu.cn

[1] National Synchrotron Radiation Laboratory, School of Nuclear Science and Technology, University of Science and Technology of China, Hefei 230029, China

[2] Laboratory Medical Optical and Mass Spectrometry, Center of Medical Physics and Technology, Hefei Institutes of Physical Science, Chinese Academy of Sciences, No. 350, Shushanhu Rd., Hefei 230031, China

[3] Laboratory of Atmospheric Physico-Chemistry, Anhui Institute of Optics and Fine Mechanics, Chinese Academy of Sciences, Hefei 230031, China

[4] School of Environmental Science and Optoelectronic Technology, University of Science and Technology of China, Hefei 230026, China

1 Introduction

Cyclohexene, which is emitted from both natural and anthropogenic sources, is one of the most abundant cyclic alkenes in urban areas, which are known to produce aerosols upon atmospheric oxidation [1]. Previous studies have shown that the major pathway to aerosol formation for many cyclic alkenes such as cyclohexene involves reaction with O_3 rather than with the OH radical [2, 3]. The kinetics, gas-phase, and particle-phase products of the O_3–cyclohexene reaction have been the subject of many investigations over a long period of time (see, for instance, Refs. [4–10], and the references therein). In general, the chemical composition of the particle-phase products of this reaction, i.e., the secondary organic aerosol (SOA), has often been analyzed using off-line techniques such as gas chromatography–mass spectrometry (GC–MS), with the SOA first being collected on the filter and then treated using complex sample preparation procedures such as elution, extraction, and concentration. However, it is well known that a variety of components of organic aerosols cannot be resolved using traditional GC–MS [11, 12], and

 Springer

the related time-consuming analytical protocols are prone to contamination and losses during the collection and extraction steps. Additionally, analyses based on traditional MS methods utilizing laser photoionization or electron impact ionization generally suffer from fragmentation of the molecular ions, which generate a bewildering number of mass peaks that are extremely hard to identify.

Recently, in an effort to fulfill the need for investigation of the organic constituents emerging from atmospheric oxidation in laboratory studies, aerosol mass spectrometers (AMS) employing vacuum ultraviolet (VUV) photons generated using synchrotron radiation (SR) as the ionization source have been developed and have been used for online characterization of the composition of SOA [13–15]. The "soft" VUV photoionization minimizes the fragmentation in the particle mass spectra, allowing direct identification of the organics within the aerosol via their molecular ions as well as via their ionization energies (IEs), which are obtained from the photoionization efficiency curves (PIEs) [15–17].

The coupling of synchrotron radiation photoionization mass spectrometry with a smog chamber has been proven to be a powerful tool to characterize the composition of SOA and could provide important structural information that is difficult to obtain using other techniques [15, 18, 19]. In this study, we have reinvestigated the cyclohexene–ozone system in an attempt to shed light on the discrepancies existing in the literature concerning the low molecular weight components in the SOA produced in this system. The compounds in the aerosol phase were investigated online using a recently developed thermal desorption/tunable vacuum ultraviolet photoionization time-of-flight aerosol mass spectrometer (TD-VUV-TOF-PIAMS) combined with a custom-built smog chamber. In addition, an off-line method employing filter collection coupled with TD-VUV-TOF-PIAMS was tested to probe the composition of the SOA produced by cyclohexene ozonolysis for the first time, which may have potential applications in both field and laboratory measurements of atmospheric aerosols.

2 Experimental

The experimental apparatus was composed of a sampling system, a main smog chamber system, and the detection system. Detailed descriptions of the chamber facility used in this study have been reported previously [15, 18, 19], and only a brief summary is given here. Three different types of experiments, namely, online, off-line, and blank experiments, were performed in a custom-built collapsible $\sim$ 1500-L fluorinated ethylene propylene (FEP) Teflon (Shanghai Plastics Research Institute,

Shanghai, China) cylinder bag at 1 atm and ambient temperature ($\sim$ 298 K) without using seed particles. Prior to each experiment, the chamber was continuously flushed for at least 2 h with purified compressed dry zero air, which contained no particles and no detectable reactive hydrocarbons, and illuminated with 12 fluorescent black lamps to ensure that the concentrations of residual particles and volatile organic compounds (VOCs) were lower than the detection limits of the experiments. The zero air was dried using a heatless air dryer (CKD HD-0.5, CKD Co., Ltd., Komaki, Japan). The humidity and temperature were continuously monitored during the experiments using a humidity–temperature sensor (Vaisala, HMT330, Finland). The relative humidity of the chamber was maintained at about 15% for all the experiments. During the experiments, the black lamps were switched off and the collapsible bag was covered with a thick aluminum shell to avoid possible photochemical reaction of the VOCs. In the online experiment, ozone ($\sim$ 5 ppm) was injected into the chamber by passing pure oxygen through an ozone generator (Pacific Ozone Co., USA), and its concentration was monitored online using an ozone analyzer (Model 49i, Thermo Fisher Scientific, USA). Equimolecular cyclohexene (99%, TCI) was injected into a glass bulb and flushed into the chamber by a stream of purified air through Teflon lines. The size distribution and number concentration of the SOA particles in the chamber were measured with a differential mobility analyzer (DMA; Model 3081, TSI) and an ultrafine condensation nucleus counter (CNC; Model 3776, TSI).

After initiation of the reaction, the aerosols produced in the chamber were sampled through a 6-mm conductive silicone tube and introduced into the TD-VUV-TOF-PIAMS developed at the Atomic and Molecular Physics Beamline (BL09U) of the National Synchrotron Radiation Laboratory (NSRL) in Hefei, China. The design of the TD-VUV-TOF-PIAMS is similar to the instrument developed at the Chemical Dynamics Beamline at the Advanced Light source [15], and its functionality has been described elsewhere [18, 20]. Briefly, the aerosols were introduced into the source chamber via an aerodynamic lens system, which provides high transmission efficiency for particles with diameters ranging from 0.1 to 1.5 μm. At the lens output, the focused particle beam then passed through the differential chamber and was accelerated by the gas expansion. Once transported into the ionization region of the detection chamber, the particles collided with a temperature-controlled cartridge heater and were promptly thermally vaporized at an appropriate temperature. Subsequently, the nascent vapor plume was irradiated with the tunable VUV light produced by an undulator at Beamline BL09U of NSRL, which generated photons with energies of 7.5–22.5 eV. The photon energy resolution can be obtained using the multistage photoionization chamber system

described previously [21]. In the present experiments, the resolving power ($E/\Delta E$) of the 370 grooves mm^{-1} grating as determined from the line shapes of the Rydberg resonances of Ar^+ was above 2000 when the slit width was adjusted to 80 μm. Because the IE values of most organic species lie below 11 eV, photons with an energy of 11.5 eV were used in the present study to ensure the organic vapor could be ionized with minimal excess internal energy and therefore minimal fragmentation. The ions formed in the ionization region were then periodically extracted by a pulsed repeller voltage ($-$ 165 V, 2.5 μs pulse width and 18 kHz repetition rate) that was triggered by a pulse generator (DG 535; Stanford Research System Inc., Sunnyvale, CA, USA). The pulsed ions were subsequently transferred through the focusing lenses (900 V focus voltage) and drift area ($-$ 1000 V accelerating potential) before being reflected by the retarding lenses (460 V reflecting voltage). Finally, the ions were collected and detected by a two-stacking microchannel plate (MCP) detector. The resulting ion signals were passed through a preamplifier (VT120C; EG&G ORTEC, Oak Ridge, TN, USA) and collected with a multichannel scaler (FAST Comtec p7888, Germany) to produce the photoionization mass spectra. The mass resolution of the TD-VUV-TOF-PIAMS was measured using the mass spectrum of urea particles, which were produced by atomizing a solution of 0.3 g urea in 300 ml ethanol. The mass resolving power M/ΔM was determined to be about 800 at m/z 60, which allowed for the characterization of SOA mass spectra in our experiments with unit mass resolution.

The off-line experiments were conducted in the same chamber with the initial concentration of both cyclohexene and O_3 being $\sim$ 1 ppm. After the introduction of O_3 and cyclohexene into the chamber, the generated particles were continuously analyzed by TD-VUV-TOF-PIAMS as well as by the scanning electrical mobility spectrometer (SMPS), which was composed of the DMA and CNC mentioned above. After the completion of the reaction, the aerosol was collected on a quartz-fiber filter with a 47 mm diameter and 0.45 μm pore size, which had been pre-backed at 550 °C for 12 h before sample collection. The aerosol was collected using a sample pump at a flow rate of approximately 20 L min^{-1} for 50 min, resulting in a total sampling volume of $\sim$ 1 m^3. When the collection was finished, the filter was placed into a sample vial filled with 50 ml of HPLC-grade acetone, which has been proven to be an excellent solvent for SOA [18]. The sample vial was wrapped in foil to prevent photolysis and left for 1 h before being sonicated for 30 min. The solution was then filtered using a 0.45-mm PVDF syringe filter and subsequently transferred into a custom-built atomizer that was structurally similar to the commercial Constant Output Atomizer (TSI, Inc., model 3076) but with a smaller volume.

Polydisperse and dry particles were prepared by atomizing the solution with N_2 at a pressure of 1 atm and dried using a diffusion dryer filled with silica gel. Finally, the particles were introduced into the TD-VUV-TOF-PIAMS for mass spectral analysis through conductive tubing T-junction, with the excess aerosol being exhausted.

3 Results and discussion

In the present work, we present both online and off-line mass spectrometric studies of the SOA formed from the ozonolysis of cyclohexene in a smog chamber. Before the introduction of the reactants, the entire sampling system and the chamber were purged at least thrice using compressed zero air. Figure 1a depicts the photoionization mass spectrum of the zero air in the chamber before the
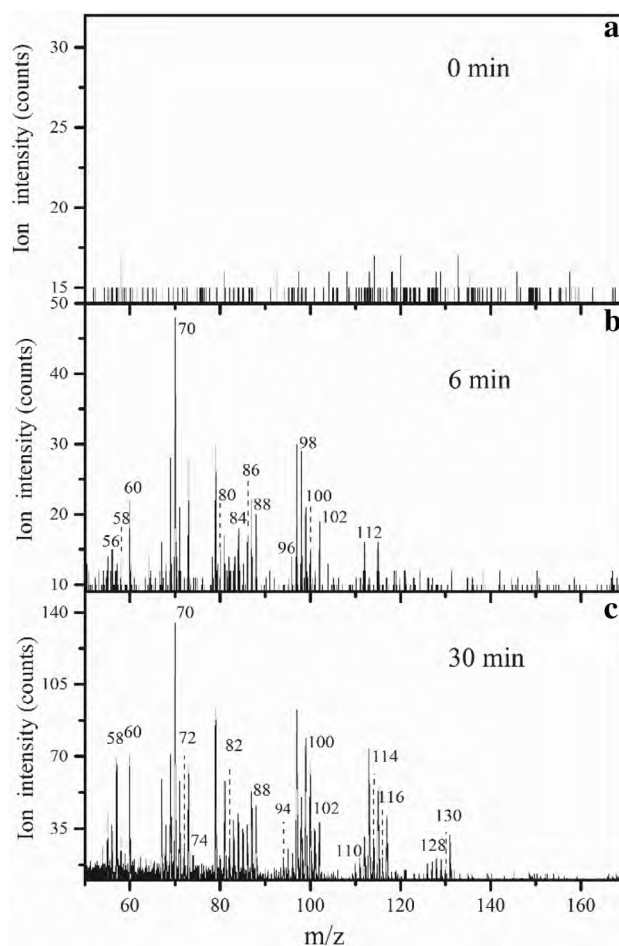

Fig. 1 TD-VUV-TOF-PIAMS mass spectra of **a** zero air (background) before the injection of cyclohexene and ozone, **b** 6 min after the injection of cyclohexene and ozone, and **c** 30 min after the injection of cyclohexene and ozone. All the mass spectra were obtained at 11.5 eV with an acquisition time of 100 s for each spectrum

injection of the reactants at 11.5 eV; the higher-order harmonics were suppressed by the rare-gas harmonic filter. Because almost all the hydrocarbons and particles in the air were eliminated by the zero-air generator and the high-efficiency particulate arresting (HEPA) filter, the mass spectrum shown in Fig. 1a was remarkably clean, and no obvious mass peaks were observed in the range of 50–170 Da. The mass spectra were recorded from 0 to 300 Da during the experiments. Since no product with an m/z below 50 has been reported in previous studies, and no mass peak with an m/z larger than 170 has been found in our experiments, in the following discussion, we present the photoionization mass spectrum only in the mass range of 50–170 Da. In this work, the vaporization temperature of the heated tip was set at 400 K to maximize the molecular ion signal and to minimize fragmentation caused by providing excess internal energy to the molecules.

Once cyclohexene and ozone were injected into the smog chamber, the reaction immediately started, and the SOA particles reached a detectable size within a few minutes of injection, as characterized by the SMPS. Figure 2a shows the time-dependent mass concentration of the SOA particles resulting from the ozonolysis of cyclohexene after ozone injection. Each point in the figure represents the mass concentration of particles measured by the SMPS, which was calculated from the size distributions and particle density. The mass concentration of the particles increased rapidly after the injection of ozone, reached a maximum at about 40 min, and then decreased, probably

due to wall loss and deposition. The size distribution of the particles measured 40 min after the ozone injection is shown in Fig. 2b. The mean diameter of the particles was determined to be ~ 435 nm, and the particle number concentration was ~ 1.08×10^4 cm^{-3}.

Figure 1b shows the mass spectrum of the particle components sampled directly from the chamber after 6 min of reaction with a data acquisition time of 100 s. It is obvious that many mass peaks are presented in Fig. 1b, including ions at m/z 56, 58, 60, 70, 80, 84, 86, 88, 96, 98, 100, 102, and 112, with the most intense peak at m/z 70. These ion signals disappeared when the vaporization temperature was set to 298 K or when the sampling was stopped while the vaporization temperature was set to 400 K. In addition, the cyclohexene ozonolysis SOA products filtered using a HEPA filter (99.99% retention efficiency for particles and droplets > 10 nm) were analyzed online using TD-VUV-TOF-PIAMS when the vaporization temperature was maintained at 400 K, and no obvious mass peak was observed. It is thus confirmed that these mass peaks do indeed arise from the SOA particles rather than from the gas phase or from background contamination. It is remarkable that most of the peaks were observed at low molecular weight, unlike in previous online measurements using a thermal desorption particle beam mass spectrometer (TDPBMS) or laser-ionization single-particle aerosol mass spectrometer (LISPA-MS), in which a variety of fragments (below 50 Da) were observed [6, 9]. By comparing the mass spectra measured at different reaction times, Ziemann found that the composition of the SOA produced in the ozone–cyclohexene system changes significantly over the course of the reaction [6]. In this study, the particle products were measured every 2 min by the TD-VUV-TOF-PIAMS after the injection of the reactants. As shown in Fig. 1c, most of the mass peaks observed in Fig. 1b became more intense after 30 min of reaction, and new products at m/z 72, 82, 94, 110, 114, 116, 128, and 130 were detected. The main SOA products observed in this study and the corresponding references are listed in Table 1.

As mentioned above, the reaction mechanism, gas-phase, and particle-phase products generated in the reaction of cyclohexene and ozone have been studied by many different techniques. The species at m/z 56 was also detected by Hamilton and colleagues using comprehensive gas chromatography with time-of-flight mass spectrometry (GC × GC-TOF/MS) and was assigned as 2-propenal, whose formation mechanism still remains unclear [8]. The products at m/z 58 and 60 present at the beginning of the reaction have been previously detected in negative-ion spectra, but their structure cannot be identified. One possible candidate for the m/z 58 product is glyoxal, which is the precursor of oxoacetic acid and is speculated to be
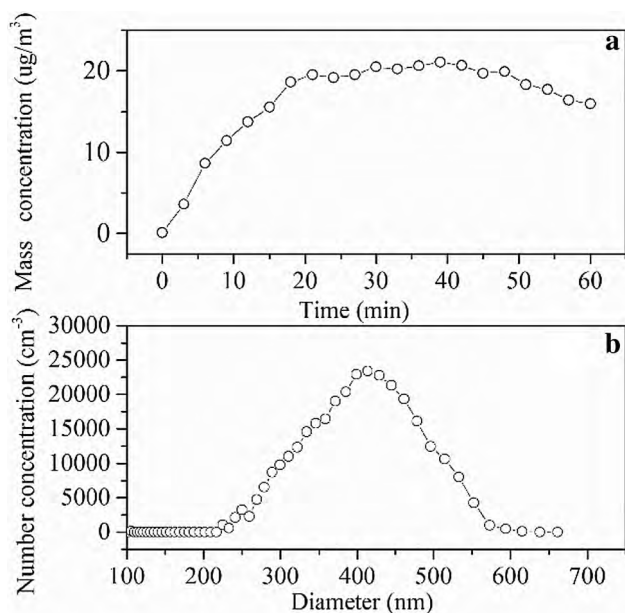

Fig. 2 a Time-dependent mass concentration of the SOA particles resulting from the ozonolysis of cyclohexene. **b** Particle size distribution of the SOA particles measured by the SMPS after 40 min of cyclohexene–ozone reaction

Table 1 The main particle products of the ozonolysis of cyclohexene observed by TD-VUV-TOF-PIAMS
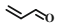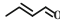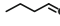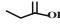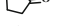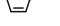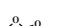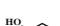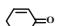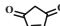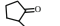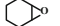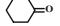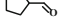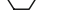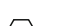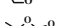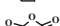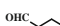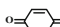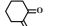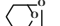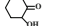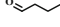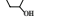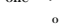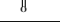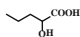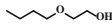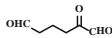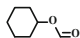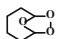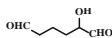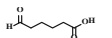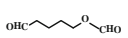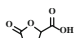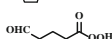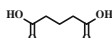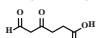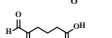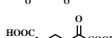
m/z	Formula	Trivial name	Structure	References
56	C_3H_4O	2-Propenal		[8]
70	C_4H_6O	2-Butenal		[8]
72	C_4H_8O	Butanal		[8, 9]
74	$C_3H_6O_2$	Propanoic acid		[8, 9]
	$C_4H_{10}O$	Butanol		[8]
82	C_5H_6O	Cyclopentenone		[8]
84	$C_4H_4O_2$	2(5H)-Furanone		[8]
	C_5H_8O	Cyclopentanone		[8]
86	$C_5H_{10}O$	Pentanal		[5, 7, 8]
	$C_4H_6O_2$	Butanedial		[5, 8, 9]
	$C_4H_6O_2$	Dihydro-2(3H)-furanone		[8]
88	$C_4H_8O_2$	2-Butene-1,4-diol		[8]
	$C_4H_8O_2$	4-Hydroxy-1-butanal		[5]
	$C_4H_8O_2$	Butanoic acid		[8, 9]
96	C_6H_8O	Cyclohexen-2-one		[8]
	$C_5H_4O_2$	Cyclopentendione		[8]
98	$C_6H_{10}O$	2-Methyl-cyclopentanone		[8]
	$C_6H_{10}O$	7-Oxobicyclo[4.1.0]heptane		[8]
	$C_6H_{10}O$	Cyclohexanone		[8]
	$C_6H_{10}O$	2-Hexenal		[8]
	$C_6H_{10}O$	Cyclopentane carboxaldehyde		[8]
100	$C_6H_{12}O$	2-Hexanone		[8]
	$C_6H_{12}O$	Hexanal		[8]
	$C_6H_{12}O$	Cyclohexanol		[8]
	$C_5H_8O_2$	1,5-Pentanedial		[4, 5, 7, 9]
	$C_5H_8O_2$	Tetrahydro-2H-pyran-2-one		[8]
	$C_5H_8O_2$	Dihydro-5-methyl-2(3H)-furanone		[8]
	$C_4H_4O_3$	2,5-Dihydro-furandione		[8]
102	$C_5H_{10}O_2$	Pentanoic acid		[8]
	$C_4H_6O_3$	4-Oxo-butanoic acid		[5, 9]
110	$C_6H_6O_2$	2-Cyclohexen-1,4-dione		[8]
112	$C_6H_8O_2$	1,2-Cyclohexadione		[8]
114	$C_6H_{10}O_2$	6,8-Dioxabicyclo[3.2.1]octane		[8]
	$C_6H_{10}O_2$	2-Dydroxy-cyclohexanone		[8]
	$C_6H_{10}O_2$	2-Oxepanone		[8]
	$C_6H_{10}O_2$	Hexanedial		[4, 5, 7, 8, 9]
	$C_6H_{10}O_2$	Dihydro-2H-pyran-2,6-(3H)-dione		[8]
116	$C_6H_{12}O_2$	1,2-Cyclohexandiol		[8]
	$C_6H_{12}O_2$	Hexanoic acid		[8]
	$C_5H_8O_3$	5-Oxo-pentanoic acid		[6, 7, 9]
118	$C_4H_6O_4$	Succinic acid		[5, 6, 8, 9]

Table 1 continued

	$C_5H_{10}O_3$	2-Hydroxy pentanoic acid		[6]
	$C_6H_{14}O_2$	2-Butoxyethanol		[8]
128	$C_6H_8O_3$	2-Oxo-pentanedial		[7]
	$C_7H_{12}O_2$	Formic acid cyclohexyl ester		[8]
130	$C_6H_{10}O_3$	7,8,9-Trioxabicyclo[4.2.1]nonane		[7]
	$C_6H_{10}O_3$	2-Hydroxyglutaraldehyde		[7]
	$C_6H_{10}O_3$	6-Oxo-hexanoic acid		[4, 6, 8, 9]
	$C_6H_{10}O_3$	5-Oxo-pentyl formate		[6]
	$C_5H_6O_4$	5-Oxotetrahydro-furan-2-carboxylic acid		[8]
132	$C_5H_8O_4$	5-Oxoperoxypentanoic acid		[6]
	$C_5H_8O_4$	Glutaric acid		[4, 5, 6, 8, 9]
144	$C_6H_8O_4$	4,6-Dioxohexanoic acid		[8]
	$C_6H_8O_4$	5,6-Dioxohexanoic acid		[9]
160	$C_6H_8O_4$	2-Oxoadipic acid		[9]

formed through further reaction of the excited intermediate $OHC(CH_2)_3CHCHOOH$ generated by isomerization of the Crigee biradical [5]. In the case of the m/z 60 product, to the best of our knowledge, the only plausible candidate is acetic acid, which has been detected in the gaseous phase [4]. The strongest ion signal at m/z 70 in Fig. 1b, c was identified as 2-butenal based on a previous study [8]. The product with the molecular weight of 72 detected by both online LISPA-MS and off-line GC × GC-TOF/MS method was reported to be butanol [8, 9]. However, its formation mechanism is not well understood. Based on previous studies, the species at m/z 74 were assigned as propanoic acid and butanol. It is interesting that some cyclic compounds with molecular weights of 82, 110, and 112, which previously had only been detected by the GC × GC-TOF/MS method, were also observed in our experiments; these were assigned as cyclopentenone, 1,4-cyclohexen-2-dione, and 1,2-cyclohexanone, respectively. As far as we know, the formation of these species is hard to rationalize from known cyclohexene ozonolysis pathways, and they may be formed through reactions within the aerosol phase, which are still poorly understood. Two other isobaric compounds with a cyclic structure, 2(5H)-furanone and cyclopentanone, were detected both in this investigation and in a previous study [8]. On the basis of known reaction mechanisms, we speculated that the latter may be generated by cyclization of the biradical $CH_2(CH_2)_3CO$, which is formed from the decomposition of the primary ozonide. It has been proposed that the intermediate produced by isomerization of the Criegee biradical can also lead to a C_4 alkyl radical

that can generate 4-hydroxy-1-butanal and butanedial through further reaction [5]. Accordingly, the products at m/z 86 and 88 detected here may be assigned as butanedial and 4-hydroxy-1-butanal, respectively. In addition, the m/z 86 products have also been identified as pentanal and dihydro-2(3H)-furanone, with the m/z 88 products being identified as 2-butene-1,4-diol and butanoic acid based on different analytical methods. For the ions at m/z 96, 98, and 100, the candidate compounds are more complicated, as listed in Table 1, in which several isobaric and/or isomeric species are given for each ion. Except for 1,5-pentanedial, all the other species have only been detected by the GC × GC method. A similar trend was found for the ions at m/z 114 and 116 presented in Fig. 1c, which were mainly composed of ring-containing compounds. These compounds cannot be detected in traditional GC–MS even coupled with newly developed derivatization methods, possibly due to its limited resolving power for complicated samples such as SOA. Among the products listed in Table 1, we noted that cyclohexanol was also detected by synchrotron photoionization measurements in the reaction between OH radicals and cyclohexene [22], indicating that it may be formed through oxidation of cyclohexene with unscavenged OH radicals in the current experiment. The species at m/z 128, which was previously detected as formic acid cyclohexyl ester, may also involve the contribution of 2-oxo-pentanedial, whose formation mechanism has been proposed, but has not been detected yet [7]. In the case of m/z 130, five different compounds have been assigned; the formation mechanisms of all these

compounds have been proposed, with the exception of 5-oxotetrahydro-furan-2-carboxylic acid.

Figure 3 depicts the time-dependent signal intensities of the SOA products at $m/z = 58$, 70, and 100 formed from the ozonolysis of cyclohexene. Each point corresponds to a mass spectrum obtained at 11.5 eV with an acquisition time of 60 s. The ion intensity was obtained by integrating the ion counts over the ion peak area. It is obvious that the signal intensities of these products increased rapidly soon after the introduction of the reactants. After a reaction time of ∼ 40 min, the intensities reached their maximum values, indicating the conclusion of the reaction, which is consistent with the conclusion of a previous study [23]. Accordingly, the aerosol collection began at that time in the off-line experiments. Meanwhile, in order to evaluate the background contamination of the present method, a blank experiment without the injection of cyclohexene was run under the same conditions used in the off-line measurement. As shown in Fig. 4a, only two peaks at m/z 58 and 59 were observed, which corresponded to the molecular ion of acetone and its isotope. Therefore, the influence of the background can be omitted in this study. Figure 4b shows the mass spectrum of the particles generated by atomizing the acetone extraction of the SOA formed in the off-line experiment. Comparing this with Fig. 1c, most of the ions detected online were also observed as shown in Fig. 4b, although the initial concentration of the reactants for the latter was decreased by a factor of 5. In addition, some new products emerged, such as the ion peaks at m/z 118, 132, 144, and 160. According to previous studies, the products with m/z 118 were assigned as succinic acid, 2-hydroxy pentanoic acid, and 2-butoxyethanol. The high molecular weight products at m/z 132, 144, and 160 were identified as multifunctional compounds of dicarboxylic acids and oxocarboxylic acids. It is necessary to clarify at this stage that the off-line method used at present is somewhat limited by the lack of complete separation between the particle- and gas-phase products. Compared with the complicated particulate products, the gaseous products generated in the ozonolysis of cyclohexene were found to be mainly composed of 1,6-hexanedial, 1,5-pentanedial, pentanal, formic acid, CO, and CO_2 [4]. Among these products, 1,6-hexanedial, 1,5-pentanedial, and pentanal have also been reported to be present in the aerosol phase. Considering the collection time of 50 min, there is a possibility that the gaseous products may be adsorbed on the filter during the sampling process. At present, however, this adsorption effect cannot be evaluated due to the lack of experimental data. In general, most of the signals observed
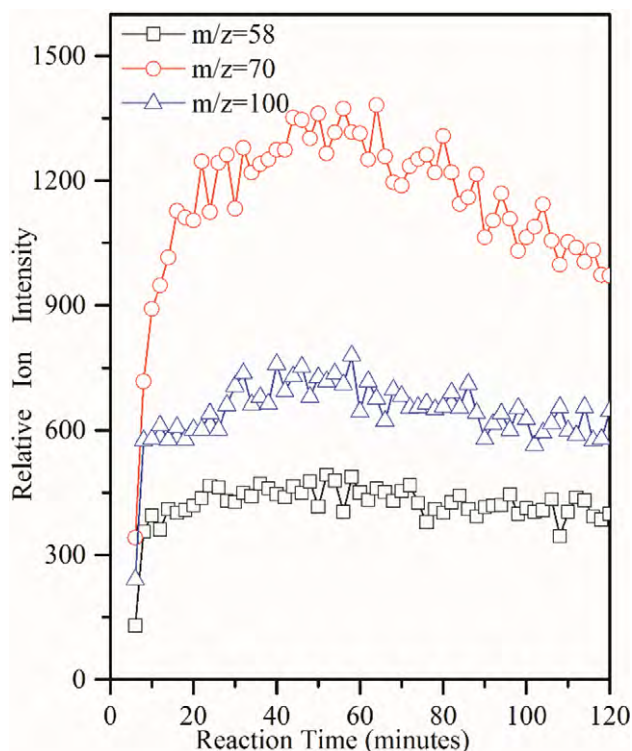
Fig. 3 (Color online) Time-dependent signal intensities of SOA products at $m/z = 58$, 70, and 100 formed from the ozonolysis of cyclohexene. The mass spectra corresponding to each point were obtained at 11.5 eV with an acquisition time of 60 s for each spectrum
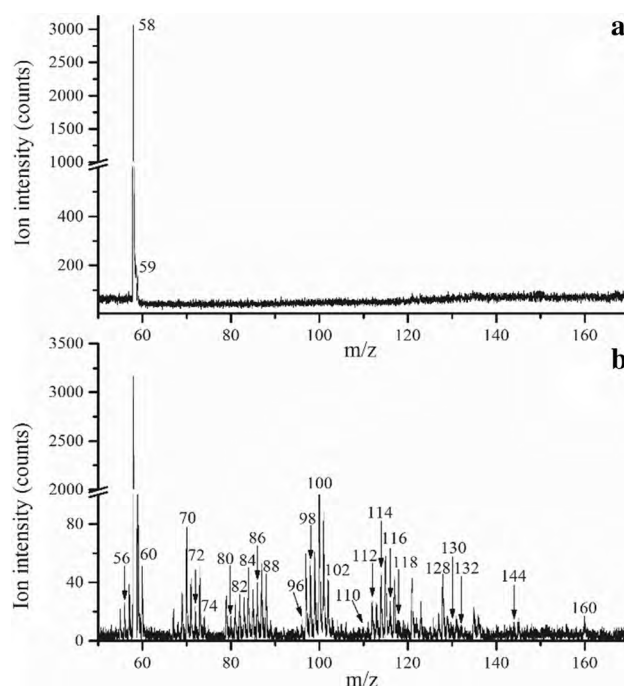
Fig. 4 TD-VUV-TOF-PIAMS mass spectra of particles generated by atomizing **a** an acetone extraction of the zero air (background) and ozone without the injection of cyclohexene and **b** an acetone extraction of the SOA formed from the ozonolysis of cyclohexene. Both the mass spectra were obtained at 11.5 eV with an acquisition time of 100 s for each spectrum

in the TD-VUV-TOF-PIAMS can be assigned based on their molecular weight and previous reports in the literature. However, some previously undetected products, such as those at m/z 80 and 94, cannot be assigned at present. One potential solution would be to carry out the experiment to determine the ionization energies of the products through PIE curves, which will be described in a forthcoming paper.

4 Conclusion

We presented the first real-time online synchrotron-based investigation of the SOA products formed from the ozonolysis of cyclohexene by employing TD-VUV-TOF-PIAMS coupled with a custom-built smog chamber. A variety of mass peaks were observed in the photoionization mass spectra at 11.5 eV, and their time-dependent signal intensities were also obtained. The analysis of the chemical composition of the SOA was carried out based on the molecular weights of the components and the identification of products in previous literature reports. The main products identified were multifunctional carbonyl compounds such as dicarboxylic acids, dialdehydes, and cyclic anhydrides. A new off-line method using filter sampling coupled with TD-VUV-TOF-PIAMS has been tested in the same reaction system. Most of the ions present in online mass spectrometry can be detected by the off-line method with a lower concentration of reactants. It is believed that this method may have potential use in the analysis of SOA components in both laboratory and field studies.

References

1. M.P. Fraser, G.R. Cass, B.R.T. Simoneit, Gas-phase and particle-phase organic compounds emitted from motor vehicle traffic in a Los Angeles roadway tunnel. Environ. Sci. Technol. **32**, 2051–2060 (1998). https://doi.org/10.1021/es970916e
2. R.J. Griffin, D.R. Cocker, R.C. Flagan et al., Organic aerosol formation from the oxidation of biogenic hydrocarbons. J. Geophys. Res. **104**, 3555–3567 (1999). https://doi.org/10.1029/1998JD100049
3. B.R. Larsen, D.D. Bella, M. Glasius, R. Winterhalter et al., Gas-phase OH oxidation of monoterpenes: gaseous and particulate products. J. Atmos. Chem. **38**, 231–276 (2001). https://doi.org/10.1023/A:1006487530903
4. S. Hatakeyama, T. Tanonaka, J.H. Weng et al., Ozone-cyclohexene reaction in air: quantitative analysis of particulate products and the reaction mechanism. Environ. Sci. Technol. **19**, 935–942 (1985). https://doi.org/10.1021/es00140a008
5. M. Kalberer, J. Yu, D.R. Cocker et al., Aerosol formation in the cyclohexene-ozone system. Environ. Sci. Technol. **34**, 4894–4901 (2000). https://doi.org/10.1021/es001180f
6. P.J. Ziemann, Evidence for low-volatility diacyl peroxides as a nucleating agent and major component of aerosol formed from

7. S.M. Aschmann, E.C. Tuazon, J. Arey et al., Products of the gas-phase reaction of O_3 with cyclohexene. J. Phys. Chem. A **107**, 2247–2255 (2003). https://doi.org/10.1021/jp022122e
8. J.F. Hamilton, A.C. Lewis, J.C. Reynolds et al., Investigating the composition of organic aerosol resulting from cyclohexene ozonolysis: low molecular weight and heterogeneous reaction products. Atmos. Chem. Phys. **6**, 4973–4984 (2006). https://doi.org/10.5194/acp-6-4973-2006
9. M. Narukawa, Y. Matsumi, J. Matsumoto et al., Real-time analysis of secondary organic aerosol particles formed from cyclohexene ozonolysis using a laser-ionization single-particle aerosol mass spectrometer. Anal. Sci. **23**, 507–512 (2007). https://doi.org/10.2116/analsci.23.507
10. M.P. Rissanen, T. Kurtén, M. Sipilä et al., The formation of highly oxidized multifunctional products in the ozonolysis of cyclohexene. J. Am. Chem. Soc. **136**, 15596–15606 (2014). https://doi.org/10.1021/ja507146s
11. W.F. Rogge, M.A. Mazurek, L.M. Hildemann et al., Quantification of urban organic aerosols at a molecular level: identification, abundance and seasonal variation. Atmos. Environ. Part A **27**, 1309–1330 (1993). https://doi.org/10.1016/0960-1686(93)90257-y
12. B.J. Williams, A.H. Goldstein, D.B. Millet et al., Chemical speciation of organic aerosol during the international consortium for atmospheric research on transport and transformation 2004: results from in situ measurements. J. Geophys. Res. (Atmos.) **112**, D10S26 (2007). https://doi.org/10.1029/2006jd007601
13. E.R. Mysak, K.R. Wilson, M. Jimenez-Cruz et al., Synchrotron radiation based aerosol time-of-flight mass spectrometry for organic constituents. Anal. Chem. **77**, 5953–5960 (2005). https://doi.org/10.1021/ac050440e
14. M.T. Baeza-Romero, F. Gaie-Levrel, A. Mahjoub et al., A smog chamber study coupling a photoionization aerosol electron/ion spectrometer to VUV synchrotron radiation: organic and inorganic-organic mixed aerosol analysis. Eur. Phys. J. D **70**, 154 (2016). https://doi.org/10.1140/epjd/e2016-70264-8
15. W.Z. Fang, L. Gong, X.B. Shang et al., Thermal desorption/tunable vacuum-ultraviolet time-of-flight photoionization aerosol mass spectrometry for investigating secondary organic aerosols in chamber experiments. Anal. Chem. **83**, 9024–9032 (2011). https://doi.org/10.1021/ac201838e
16. E. Gloaguen, E.R. Mysak, S.R. Leone et al., Investigating the chemical composition of mixed organic–inorganic particles by "soft" vacuum ultraviolet photoionization: the reaction of ozone with anthracene on sodium chloride particles. Int. J. Mass Spectrom. **258**, 74–85 (2006). https://doi.org/10.1016/j.ijms.2006.07.019
17. N.N. Wei, C.J. Hu, S.S. Zhou et al., VUV photoionization aerosol mass spectrometric study on the iodine oxide particles formed from O_3-initiated photooxidation of diiodomethane (CH_2I_2). RSC Adv **7**, 56779 (2017). https://doi.org/10.1039/c7ra11413c
18. G. Pan, C.J. Hu, Z.Y. Wang et al., Direct detection of isoprene photooxidation products by using synchrotron radiation photoionization mass spectrometry. Rapid Commun. Mass Spectrom. **26**, 189–194 (2011). https://doi.org/10.1002/rcm.5295
19. W.Z. Fang, L. Gong, Q. Zhang et al., Measurements of secondary organic aerosol formed from OH-initiated photo-oxidation of isoprene using online photoionization aerosol mass spectrometry. Environ. Sci. Technol. **46**, 3898–3904 (2012). https://doi.org/10.1021/es204669d
20. W.Z. Fang, L. Gong, X.B. Shan et al., A VUV photoionization organic aerosol mass spectrometric study with synchrotron

radiation. J. Electron Spectrosc. Relat. Phenom. **184**, 129–133 (2011). https://doi.org/10.1016/j.elspec.2010.12.004

21. S.S. Wang, R.H. Kong, X.B. Shan et al., Performance of the atomic and molecular physics beamline at the National Synchrotron Radiation Laboratory. J. Synchrotron Rad. **13**, 415–420 (2006). https://doi.org/10.1107/S0909049506030536

22. A.W. Ray, C.A. Taatjes, O. Welz et al., Synchrotron photoionization measurements of OH-initiated cyclohexene oxidation: ring-preserving products in OH + cyclohexene and hydroxycyclohexyl + O_2 reactions. J. Phys. Chem. A **116**, 6720–6730 (2012). https://doi.org/10.1021/jp3022437

23. K. Sato, Chemical compositions of secondary organic aerosol from the ozonolysis of cyclohexene in the absence of seed particles. Chem. Lett. **34**, 1584–1585 (2005). https://doi.org/10.1246/cl.2005.1584